 doi:10.20944/preprints201810.0528.v1

Article

Effects of Concentration Percentages of PCL/AGNO3/ZNO on Electrical Properties of Nanofiber Composites Produced by Using Co-Axial Electrospinning

Umit Kemalettin Terzi[1,3,*], Oguzhan Gunduz[2,3]

[1] Department of Electric-Electronic Engineering, Faculty of Technology, Marmara University, Goztepe Campus, 34722, Istanbul, Turkey; terzi@marmara.edu.tr
[2] Department of Metallurgical and Materials Engineering, Faculty of Technology, Marmara University, Goztepe Campus, 34722, Istanbul, Turkey; oguzhan.gunduz.09@alumni.ucl.ac.uk
[3] Nanotechnology and Biomaterial Research and Implementation Centre, Marmara University, Goztepe Campus, 34722, Istanbul, Turkey
* Correspondence: terzi@marmara.edu.tr or ukterzi@gmail.com (U.K.T); Tel.: +90-542-314-9336

Abstract: Nanofibers appearing functional properties show a great promise as allowing constituents for a wide range of medical applications. In this work, Polycaprolactone (PCL), Silver Nitrate ($AgNO_3$) and Zinc Oxide (ZnO) were used for fabrication of nanofiber composite material by co-axial electrospinning (CAE) process. 5, 10, and 15 wt. % concentrations of PCL were utilized and different amount of $AgNO_3$ and ZnO were used in entire samples. Morphological analyses of the electrospun nanocomposites were done by scanning electron microscopy (SEM) and $AgNO_3$, ZnO and PCL materials' functional groups were determined by Fourier Transform Infrared Spectroscopy (FTIR). Before co-axial electrospinning, physical properties such as liquid state ac conductivity, density and viscosity were measured for all solutions. Capacitance (C_P) and D-factors ($tan\delta$) of nanocomposite materials are measured for the frequency range of 20Hz – 3MHz and the solid state alternating current (ac) conductivity, permittivity (ε′) and dielectric loss (ε′′) were calculated for all solutions after co-axial electrospinning. Effects of concentration percentages of PCL and $AgNO_3$ on real and imaginary parts of dielectric constant and solid state ac conductivity have been analyzed and comparisons have been made by the results obtained.

Keywords: biocomposites, nanomaterials, measurement, electrical properties, electrospinning

1. Introduction

With the rapid improvement of nanotechnology over the last two decades, significant progress has been made not only in fabrication and measurement of nanostructures but also for their functional purposes. As a crucial one-dimensional nanostructure, nanofibers have a particularly very high specific surface area and therefore nanofiber membranes are very porous with superb pore interconnectivity. According to literature, it can easily be seen that electrospinning process is reported for the fabrication of nanofibers for different purposes. Electrospinning is a basic and versatile process for the production of polymers, composite and ceramic fibers. Nanofibers polymer materials fabricated by electrospinning have obtained immense research interest because of their functional properties, such as high surface-area-to-volume and aspect ratios. There are some alternative operation types of electrospinning and one of them is co-axial needle electrospinning. The principles, method details and biomedical engineering applications of coaxial-needle electrospinning have been stated in detail in the literature [1].

 doi:10.20944/preprints201810.0528.v1

This Co-axial electrospinning (CAE) process has attracted great interest from researchers because of its novel molecular structure and remarkable electronic properties and its promising applications in photosensitizers, gas sensor devices, stabilizers as functional materials and biochemistry and biomedical engineering applications. Although several research papers have been published in recent years, CAE processing is a relatively new technique but there are many applications in this technique which need to be researched. Among various types of biomaterials, Polycaprolactone (PCL) has many advantages such as biocompatibility, biodegradability, low cost and ease of control for fabricating process in electrospinning [2, 3]. Zinc oxide (ZnO) a wurtzite n-type semiconductor, which is in its varying forms with unique properties, such as, direct band gap (3.37 eV), high exciton binding energy (60 meV), and good resistivity (10−3 to 105 Ωcm) is amongst the widely explored functional metal oxide semiconductors [4]. Virovska et al. have shown that Electrospun poly(lactic acid) (PLA) was surface functionalized with nanosized ZnO leading to nonwoven mats in which ZnO was coated either on the surface or within the bulk, the former exhibiting higher photocatalytic activity [5]. Dobrzański et. al have stated that $AgNO_3$ leads to higher electrical conductivity of the solution along with the increasing fraction of silver nitrate additives relative to the initial solution. They also showed that the fraction of silver nitrate affects the surface area of the nanofibers obtained [6]. Functional polymer nanocomposites have the ability to meet these requirements and the use of various conductive precursors, such as metallic, ceramic, nanoparticles, thin films and nanofibers have been significantly explored and revealed to improve the conductivity and dielectric properties. However, insufficient research has been done on the dielectric properties of the composites enhanced by these nanocomposites.

By using dielectric spectroscopies, Kaya et al. examined the mixing temperatures' effects on dielectric properties of poly(methyl methacrylate) (PMMA)-pristine bentonite nanocomposites. They observed that the permittivity decreases and the dielectric relaxation displaces towards the lower frequencies by lowering the mixing temperature [7].

Kaya et al. investigated the dielectric and electric properties of Poly(vinyl imidazole)–Na–Bentonite composite. Conductivity was increased at 25°C according to the studies done on the current and voltage. From the capacitive measurements it can be concluded that the samples show typical dielectric behavior. Alternating current conductivity and loss factors are also high, depending on maximum interactions at 25°C [8].

In this work, the goal is to analyze the effects of concentration percentages of PCL and $AgNO_3$ on electrical properties of PCL/$AgNO_3$/ZnO nanofiber composites produced by using CAE processing. To observe the effects of concentration percentages of PCL and $AgNO_3$ on electrical properties of nanofiber composites, nine different samples were prepared with three different concentration percentages and dielectric spectroscopy was used to obtain information about interactions. Behavior of a dielectric can be studied through the real part (ε') and the imaginary part (ε'') of the dielectric constant and behavior of conductivity (σ*) can also be studied through the real part(σ') and the imaginary part (σ'') of the ac conductivity.

2. Materials and Methods

2.1 Preparation of PCL/$AgNO_3$/ZnO Composite Solutions

Polycaprolactone (PCL) is selected as a biopolymer material. The average molecular weight of PCL (M_w) was 80000 g/mol and it was purchased from Sigma-Aldrich and used with no extra treatment or purification. A solution of PCL was prepared with various concentrations and the percentages of solution concentration were 5, 10 and 15 wt. %. PCL was dissolved in Tetrahydrofuran (THF) and Dimethylformamide (DMF) mixture with a constant w/w 1:1 ratio and all of these solutions were stirred with a magnetic stirrer at 40^{0}C for 2 hours. The purity of the THF and DMF is 99%. $AgNO_3$ and ZnO are selected as dielectric property agents. ZnO was purchased from Sigma-Aldrich and the average molecular weight of ZnO (M_w) was 81.37 g/mol. $AgNO_3$ was purchased from Merck and average molecular weight of $AgNO_3$ was 168.87 g/mol. The percentages of $AgNO_3$ solution concentrations were 0.5 wt. %, 1 wt. % and 2 wt. % and the percentages of ZnO

 doi:10.20944/preprints201810.0528.v1

solution concentration were 5 wt. %. ZnO and $AgNO_3$ were dissolved in THF and DMF mixture with a constant w/w 1:1 ratio and all of these solutions were stirred with the magnetic stirrer at 40^{0}C for 3 hours.

2.2 Co-axial Electrospinning of PCL/$AgNO_3$/ZnO Composite Nanofibers

Samples were prepared in different concentrations using polymer and dielectric properties agent solutions and detailed information about contents of the nine samples have been listed in Table 1 and also supported with co-axial electrospinning parameters.

Table 1. The sample codes for each different polymer concentrations and solution properties of prepared 9 samples before co-axial electrospinning process.

Sample No	Material Compositions	Feeding Speed (ml/h)	Distance Between Collector and Needle (cm)	Applied Voltage (kV)	Humidity (g/m^3)	Temperature (°C)
S1	PCL (5wt.%)	0.01	9	25.9	58.3	26.9
	$AgNO_3$(0.5wt.%)	0.01				
	ZnO (5wt.%)	0.01				
S2	PCL (5wt.%)	0.01	9	21.8	63.8	24.3
	$AgNO_3$(1wt.%)	0.01				
	ZnO (5wt.%)	0.01				
S3	PCL (5wt.%)	0.02	9	23.3	60.4	27.3
	$AgNO_3$(2wt.%)	0.02				
	ZnO (5wt.%)	0.02				
S4	PCL (10wt.%)	0.02	9	20.1	60	26.7
	$AgNO_3$(0.5wt.%)	0.01				
	ZnO (5wt.%)	0.01				
S5	PCL (10wt.%)	0.02	9	23.3	63.8	27.3
	$AgNO_3$(1wt.%)	0.02				
	ZnO (5wt.%)	0.02				
S6	PCL (10wt.%)	0.02	9	18.4	60	26.7
	$AgNO_3$(2wt.%)	0.01				
	ZnO (5wt.%)	0.01				
S7	PCL (15wt.%)	0.04	9	18.6	60	26.7
	$AgNO_3$(0.5wt.%)	0.04				
	ZnO (5wt.%)	0.04				
S8	PCL (15wt.%)	0.04	9	21.7	60	24.6
	$AgNO_3$(1wt.%)	0.04				
	ZnO (5wt.%)	0.04				
S9	PCL (15wt.%)	0.05	9	21.8	50.5	27.3
	$AgNO_3$(2wt.%)	0.05				
	ZnO (5wt.%)	0.05				

As can be seen in the schematic design given in Figure 1, the solutions of PCL, ZnO and $AgNO_3$ were placed in three different plastic syringes and pinhead connected to a high voltage generator with the co-axial needle. Co-axial electrospinning was successfully carried out and PCL/$AgNO_3$/ZnO multilayered nanocomposite fibers were synthesized.

Preprints (www.preprints.org) | NOT PEER-REVIEWED | Posted: 23 October 2018 doi:10.20944/preprints201810.0528.v1

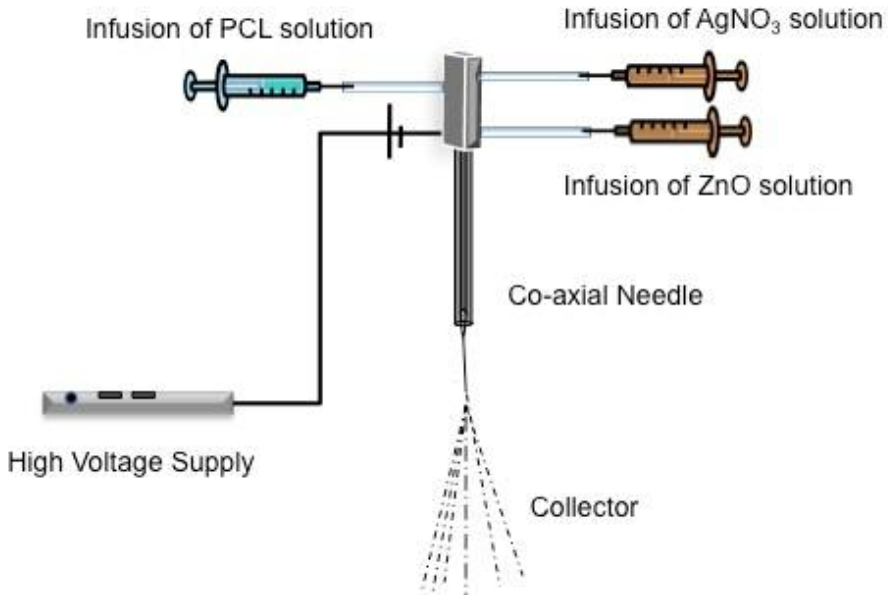

Figure 1. Schematic design of the experimental setup for co-axial electrospinning method

2.3 Characterization

2.3.1 Physical Properties of PCL, $AgNO_3$ and ZnO Solutions

Physical properties of PCL, $AgNO_3$ and ZnO solutions are studied in two sections as liquid state ac conductivity, density and viscosity and solid state ac conductivity, permittivity and dielectric loss.

2.3.1.1. Liquid state ac conductivity, density and viscosity

Physical properties of PCL (5, 10 and 15 wt. %), $AgNO_3$ (0.5, 1 and 2 wt. %) and ZnO (5 wt. %) solutions were determined. DMF and THF were used together to dissolve PCL, $AgNO_3$ and ZnO. All these samples' viscosities were measured by a viscometer (Lamy Rheology Instruments B-one Touch Viscometer). Liquid state ac conductivities of these solutions were measured with a Cond 3110 (Set 1-2CA101, Germany). In Table 2, measured viscosity, liquid state ac conductivity and density values are shown for each solution before preparing the 9 different blend solutions. In the measurement tests, 4 different examples were handled and measured to show their average numbers.

Table 2. Measured liquid state ac conductivity, density and viscosity values for different concentration of PCL, ZnO and $AgNO_3$ solutions before preparing the 9 different blend solutions.

Solution Concentrations	Viscosity (mPas)	Liquid state ac conductivity (µS/cm)	Density (g/cm^3)
5 wt. %PCL	65.4	6.18	0.9525
10 wt. %PCL	120.8	0.86	0.9728
15 wt. %PCL	182.3	0.64	0.9975
5 wt. % ZnO	45.9	3.2	0.9828
0.5 wt. % $AgNO_3$	10.1	249	0.9496
1 wt. % $AgNO_3$	10.2	457	0.9516
2 wt. % $AgNO_3$	10.5	936	0.9554

2.3.1.2. Solid state ac conductivity, permittivity and dielectric loss

For solid state alternating current conductivity, permittivity and dielectric loss measurements, samples were cut in a square shape with a side length of 20 mm. At room temperature (23^0C) and 1 Vrms potential, electrical measurements of PCL (5, 10 and 15 wt. %), $AgNO_3$ (0.5, 1 and 2 wt. %) and ZnO (5 wt. %) solutions were completed by using Impedance Analyzer (Wayne Kerr 6500 B

Preprints (www.preprints.org) | NOT PEER-REVIEWED | Posted: 23 October 2018 doi:10.20944/preprints201810.0528.v1

Precision, 20 Hz–5 MHz) and the solid state ac conductivity, the permittivity and dielectric loss values were obtained by calculations. In Table 3, the average values over a range of frequency of 20Hz to 3MHz for the permittivity, the dielectric loss and the real and imaginary parts of solid state alternating current conductivity are given for each solution after preparing the 9 different blend solutions.

Table 3. The average values over a range of frequency of 20Hz to 3MHz for the permittivity, the dielectric loss and the real and imaginary parts of solid state alternating current conductivity for each sample.

Sample No	wt.%PCL	wt.%ZnO	wt.%$AgNO_3$	Average ε′	Average ε″	Average σ′ (S/m)	Average σ″ (S/m)
S1	5	5	0.5	1.85E+00	4.37E-03	2.72E-05	8.33E-08
S2	5	5	1	2.74E-01	4.83E-04	4.02E-06	1.09E-08
S3	5	5	2	9.71E-01	2.56E-03	1.43E-05	4.25E-08
S4	10	5	0.5	7.36E-01	1.75E-03	1.08E-05	3.12E-08
S5	10	5	1	3.43E-01	7.25E-04	5.04E-06	1.37E-08
S6	10	5	2	7.78E-01	1.71E-03	1.14E-05	3.29E-08
S7	15	5	0.5	5.58E+00	1.42E-02	8.20E-05	2.47E-07
S8	15	5	1	6.49E-01	1.53E-03	9.53E-06	2.62E-08
S9	15	5	2	6.45E-01	1.52E-03	9.48E-06	2.76E-08

2.3.2 Morphological Analysis of the Electrospun Nanocomposite Fibers

The produced nanofibers' morphology was investigated with a SEM (VEGA3 SB, Tescan USA). Before the analysis, samples were coated with gold for 5 minutes. By using Olympus AnalySIS 5 (Olympus, USA), image visualization software, diameter measurements of the electrospun nanocomposites materials were done.

2.3.3 Fourier-Transform Infrared Spectroscopy (FTIR)

For the determination of the functional groups of used materials, PerkinElmer FT-IR Spectrometer Spectrum Two was used. Tests were conducted at room temperature (23°C) for all nanocomposite fiber samples in the wave number range of 400-4000 cm^{-1}, running 10 scans with a resolution of 4 cm^{-1}.

3. Results and Discussion

3.1 Morphological Characterization

Unique PCL/$AgNO_3$/ZnO nanocomposite fibers were produced to evaluate their capability for new functional opportunities with the advantage of low cost, biomedical applications and nanocomposites. Fiber diameter, bead structures, and porosity are important morphological features, and every one of them can find a different application area in healthcare engineering applications. SEM images, fiber diameter range graphics and average fiber diameter for each sample are showed in Figure 2. ZnO nanoparticles were observed in the PCL nanofibers in the samples. All the fabricated nanocomposite materials showed uniform fiber diameter distribution (Figure 2a,b). It has been shown that the diameter of nanocomposite fibers will decrease to a large extent with increasing concentration of silver nitrate nanoparticles in nanocomposite materials [9]. Average fiber diameters were 559.66 nm (Figure 2c) for all of the samples (S1 to S9).

Preprints (www.preprints.org) | NOT PEER-REVIEWED | Posted: 23 October 2018 doi:10.20944/preprints201810.0528.v1

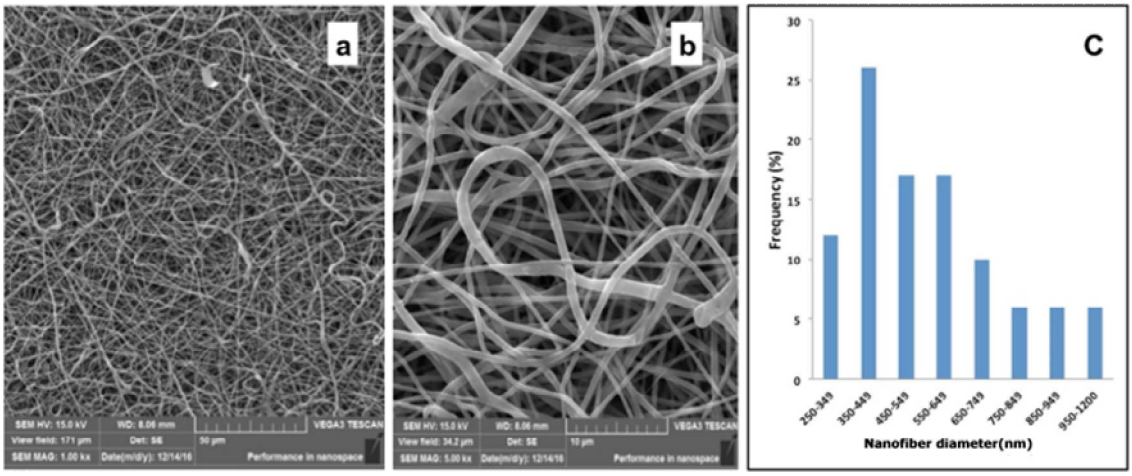

Figure 2. Scanning Electron Microscopy (SEM) images of the 5 wt.% PCL/1wt.% $AgNO_3$/5 wt.% ZnO nanocomposite fiber materials with fiber diameter frequency graphics. a) Low magnification (1000x), b) high magnification (5000x) and c) diameter distributions of nanofiber compositions

3.2 Fourier-Transform Infrared Spectroscopy (FTIR)

FTIR analyses were carried out for chemical bond analysis of PCL/$AgNO_3$/ZnO nanocomposite fiber samples (S1 to S9). In FTIR analysis, it is expected that a nanocomposite material reflects the characteristic peaks of its components.

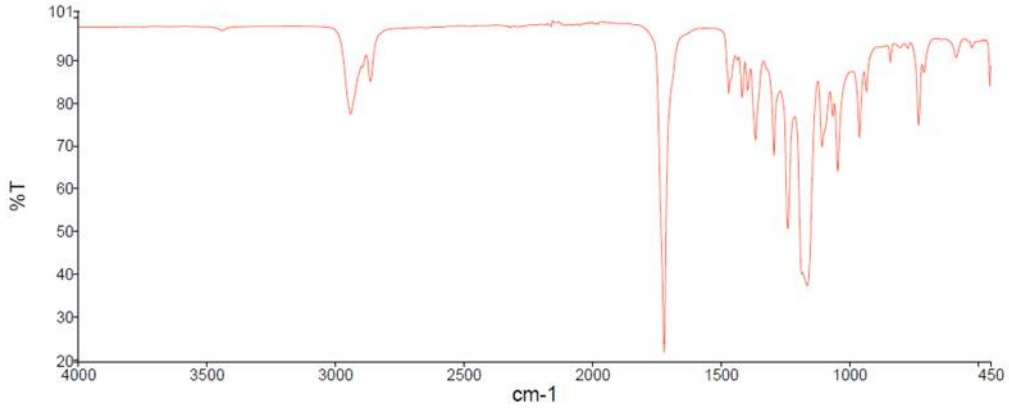

Figure 3. FTIR Spectrum of the 5 wt.%PCL/1 wt.% $AgNO_3$/5 wt.% ZnO electrospun nanocomposite material.

The infrared spectrum bands for 5 wt.% PCL/1 wt.% $AgNO_3$/5 wt.% ZnO nanocomposite sample in the wave number range of 4000 to 450 cm^{-1} can be seen in Figure 3. In all composite samples, characteristic peaks of PCL were observed including asymmetric strong bands of carbonyl stretching mode around 1722 cm^{-1}, asymmetric CH2 stretching at 2944 cm^{-1}, symmetric CH_2 stretching at 2866 cm^{-1}, C – O and C – C stretching in the crystalline phase at 1293 cm^{-1}, asymmetric COC stretching, OC – C stretching at 1168 cm^{-1}, symmetric COC stretching at 1107 cm^{-1}, and finally C – O and C– C stretching in the amorphous phase at 1046 cm^{-1} [10]. Vibrations peaks that indicate ZnO appeared as C-H stretching at 2944 cm^{-1}, strong absorption peaks were observed at 1635 and 1631 cm^{-1}, which indicates the N-H band. 1418 and 1470 cm^{-1} were assigned to C-C stretching in an aromatic group. The narrow peaks at 1065 cm^{-1} and 1046 cm^{-1} were assigned to C-N stretching in aliphatic amines. The weak absorption bands at 453 cm^{-1} indicate Zn-O stretching. The region between 400 and 600 cm^{-1} corresponds to metal oxide [11]. $AgNO_3$ showed peaks at 1651.4, 1542, 1396 and 1057 cm^{-1}. The bands obtained at 1396 and 1046 cm^{-1} are due to the presence of C-N stretching vibrations of aromatic and aliphatic amines. Molecules containing NO_2 groups, such as

Preprints (www.preprints.org) | NOT PEER-REVIEWED | Posted: 23 October 2018 doi:10.20944/preprints201810.0528.v1

nitro compounds, nitrates, and nitramines, commonly exhibit asymmetric and symmetric stretching vibrations of the NO_2 group at the 1660 to 1500 cm^{-1} and 1390 to 1260 cm^{-1} region [12].

3.3 Dielectric and Conductivity Studies

Dielectric behavior is studied through the real (ε') and imaginary (ε'') parts of the dielectric constant (ε*= ε'+ jε''). ε' is related to energy which is deposited by the external field and ε'' is related to energy loss [7, 8];

$$\varepsilon'=C_p/C_0 \, , \; \varepsilon''= \varepsilon' \tan\delta \quad (1)$$

C_0 is the vacuum capacitance and calculated by;

$$C_0= \varepsilon_0 \cdot A/d \quad (2)$$

Where;

A is area of the plates, ε_0 is the electrical permittivity of a vacuum which is equal to 8.85 $x10^{12}$ F/m and d is perpendicular spacing between plates of capacitance fixture.

Alternating current conductivity (σ*) was calculated by;

$$\sigma^*(\omega)= \sigma' + j\sigma'' = \omega\varepsilon_0\varepsilon'' + j\omega\varepsilon_0\varepsilon' \quad (3)$$

Where;

ε_0 is the free space dielectric constant and ω is angular frequency [13].

As mentioned in section 2.3.1.2., electrical measurements were completed by using Impedance Analyzer, at room temperature (23°C) at 1 V_{rms} potential over a range of frequency of 20Hz to 3MHz. To record the capacitance and tanδ data, the same procedure was repeated for each sample. First, by using Equation 2, C_0 for each sample was calculated by using thickness, area, capacitance and tanδ data of each sample for the frequency range of 20 Hz-3 MHz. After calculation of the C_0 of each sample, the calculations of ε', ε'', σ' and σ'' were done by using Equation 1 and Equation 3 respectively. After that, average value calculations over a range of frequency of 20Hz to 3MHz were done for ε', ε'', σ' and σ'' for each sample and values obtained from these procedures were presented in Table 3.

By using the data given in Table 3, graphs of average values of ε', ε'', σ' and σ'' for each sample were drawn and can be seen in Figure 4, Figure 5, Figure 6, Figure 7, respectively.

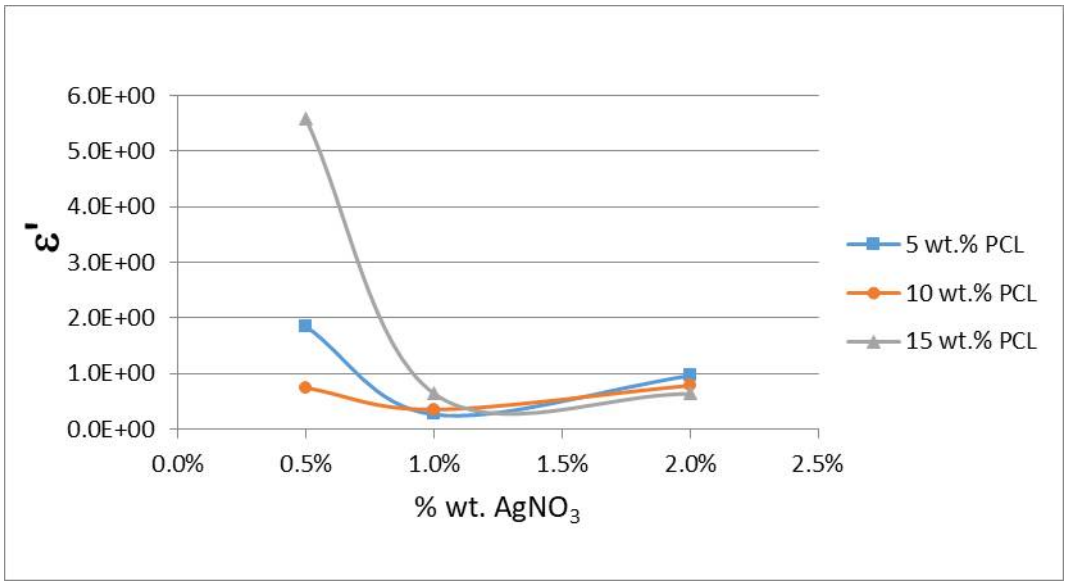

Figure 4. Graphs of average values of the real part of permittivity for 9 different blend solutions.

Preprints (www.preprints.org) | NOT PEER-REVIEWED | Posted: 23 October 2018 doi:10.20944/preprints201810.0528.v1

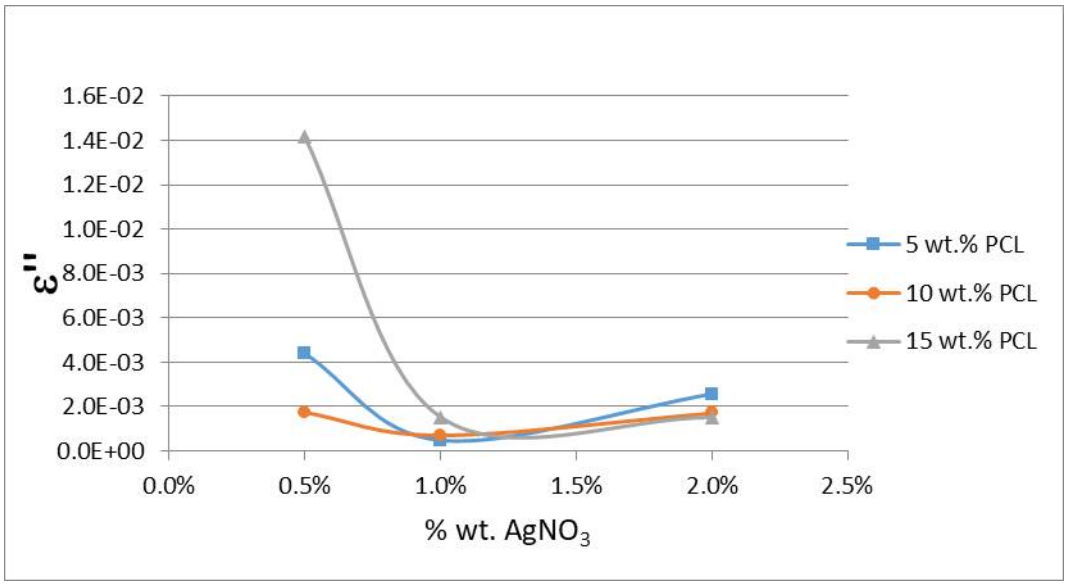

Figure 5. Graphs of average values of the imaginary part of permittivity for 9 different blend solutions.

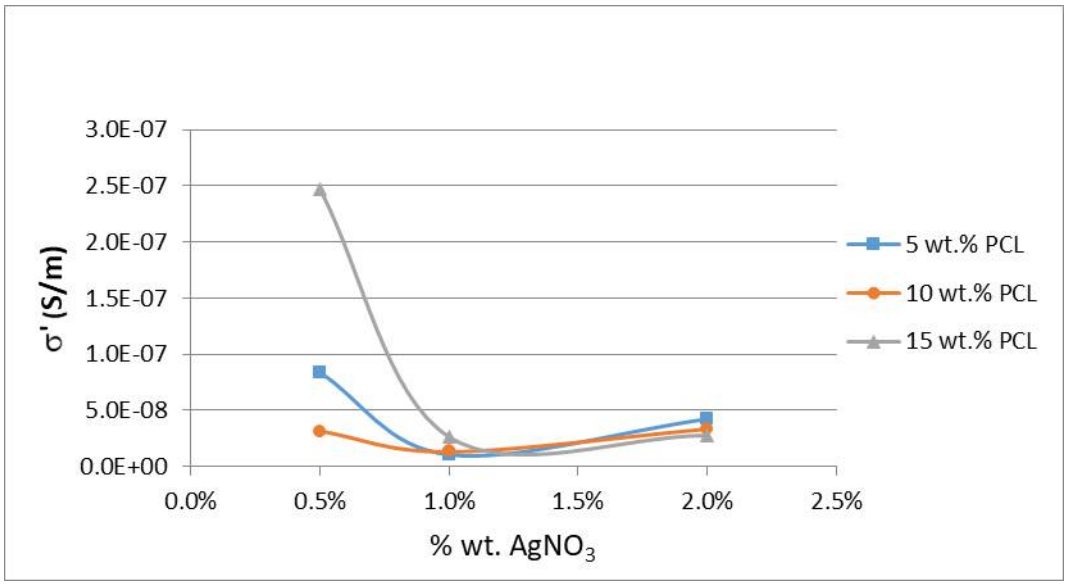

Figure 6. Graphs of average values of the real part of the alternating current conductivity for 9 different blend solutions.

Preprints (www.preprints.org) | NOT PEER-REVIEWED | Posted: 23 October 2018 doi:10.20944/preprints201810.0528.v1

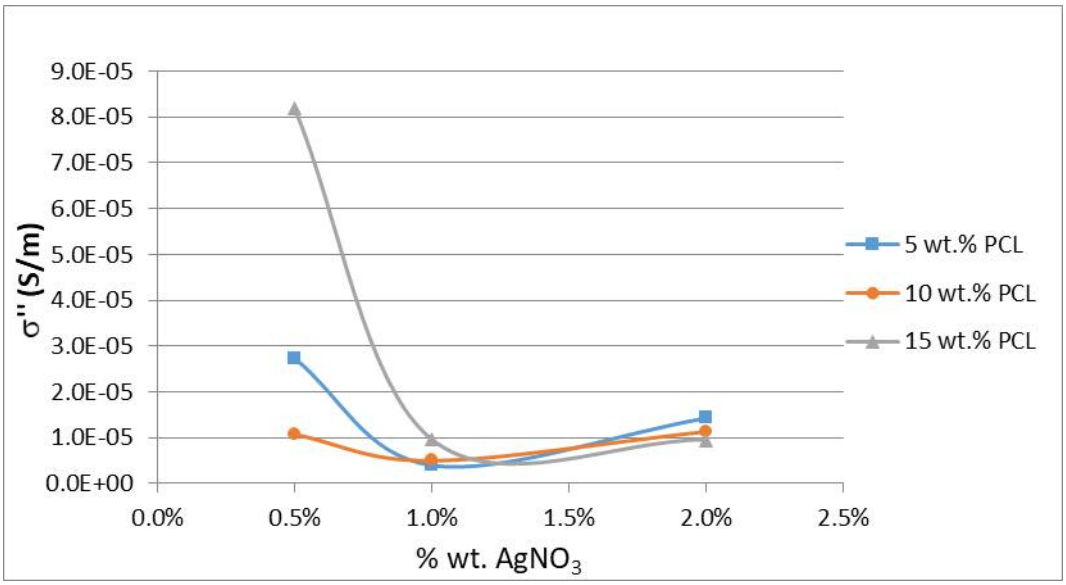

Figure 7. Graphs of average values of the imaginary parts of the alternating current conductivity for 9 different blend solutions.

For making the effects of concentration percentages of PCL and $AgNO_3$ on dielectric properties of the nanofiber composites produced by using co-axial electrospinning clear, for each concentration percentage of $AgNO_3$, the average of absolute values of differences for each PCL (5, 10 and 15 wt. %) have been calculated. Values obtained from calculations can be seen in Table 4.

Table 4. Average of absolute values of differences for PCL (5, 10, and 15 wt. %) vs. wt.%$AgNO_3$

wt.%$AgNO_3$	**Average of absolute values of differences for PCL (5, 10 and 15 wt. %)**			
	ε'	**ε''**	**σ' (S/m)**	**σ'' (S/m)**
0.5	3.228448078	0.008297431	1.44194E-07	4.74548E-05
1.0	0.249881712	0.000700123	1.02001E-08	3.6723E-06
2.0	0.217367156	0.00069333	9.88801E-09	3.20041E-06

By using data given in Table 4, graphs of the average of absolute values of differences for PCL (5, 10 and 15 wt.%) vs. wt.%$AgNO_3$ have been drawn and can be seen in Figure 8.

Preprints (www.preprints.org) | NOT PEER-REVIEWED | Posted: 23 October 2018 doi:10.20944/preprints201810.0528.v1

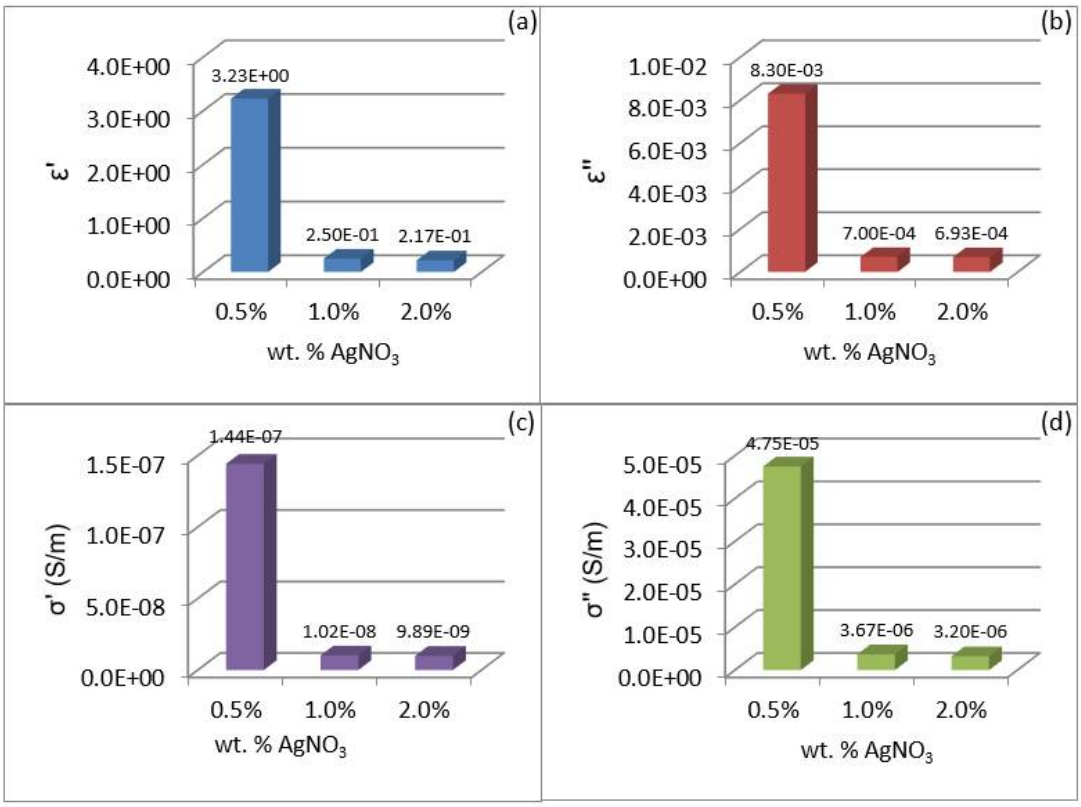

Figure 8. Graphs of the averages of absolute values of differences of (a) permittivity for PCL (5, 10 and 15 wt. %) for each concentration percentage of $AgNO_3$ (b) dielectric loss for PCL (5, 10 and 15 wt. %) for each concentration percentage of $AgNO_3$ (c) real part of alternating current conductivity for PCL (5, 10 and 15 wt. %) for each concentration percentage of $AgNO_3$ (d) imaginary part of alternating current conductivity for PCL (5, 10 and 15 wt. %) for each concentration percentage of $AgNO_3$.

As can be seen in Figure 8(a), while the concentration percentage of $AgNO_3$ changes from 0.5 % to 1%, the change in percentage of the average of absolute values of differences for the permittivity is -92.26% and when the concentration percentage of $AgNO_3$ changes from 1% to 2%, the change in percentage of the average of absolute values of differences for the permittivity is -13.01%. Similarly, as can be seen in Figure 8(b), while the concentration percentage of $AgNO_3$ changes from 0.5 % to 1%, the change in percentage of the average of absolute values of differences for the dielectric loss is -91.56% and when the concentration percentage of $AgNO_3$ changes from 1% to 2%, the change in percentage of the average of absolute values of differences for the dielectric loss is -0.97%.

The same situation is valid for the real and imaginary parts of ac conductivity. As can be seen in Figure 8(c), while the concentration percentage of $AgNO_3$ changes from 0.5 % to 1%, the change in percentage of the average of absolute values of differences for the real part of the ac conductivity is -92.93% and when the concentration percentage of $AgNO_3$ changes from 1% to 2%, the change in percentage of the average of absolute values of differences for the real part of the ac conductivity is -3.06%. Similarly, as can be seen in Figure 8(d), while the concentration percentage of $AgNO_3$ changes from 0.5 % to 1%, the change in percentage of the average of absolute values of differences for the imaginary part of the ac conductivity is -92.26% and when the concentration percentage of $AgNO_3$ changes from 1% to 2%, the change in percentage of the average of absolute values of differences for the imaginary part of the ac conductivity is -12.85%.

There is very little change in properties when either PCL or $AgNO_3$ are varied over the PCL range of 5-15% and the $AgNO_3$ range of 1-2%. From all the results explained above and figures 4,5,6,7, it clearly can be concluded that increasing the concentration percentage of $AgNO_3$ makes all

 doi:10.20944/preprints201810.0528.v1

the electrical properties studied in this paper almost independent from concentration percentage of PCL.

4. Conclusion

Within this study, 9 samples of nanocomposite material with fiber structure have been prepared by using Polycaprolactone (PCL), Silver Nitrate ($AgNO_3$) and Zinc Oxide (ZnO) and have been produced by a co-axial electrospinning method. 9 samples were examined under laboratory conditions. As seen in Figures 4,5,6,7, an increase in concentration percentage of $AgNO_3$ makes the variety of permittivity, dielectric loss and real and imaginary parts of ac conductivity of samples which are studied almost PCL independent. If these types of nanocomposite materials with fiber structure are going to be used for industrial purposes, it should be considered that concentration percentage of $AgNO_3$ will play an important role to vary the value of permittivity, dielectric loss and real and imaginary parts of ac conductivity more than concentration percentage of PCL. In other words, adjusting the concentration percentage of $AgNO_3$ will be enough to vary the value of all the electrical properties of nanocomposite materials with the fiber structure studied in this paper.

Author Contributions: U.K.T. and O.G. designed the experiments; O.G. developed and manufactured the samples. U.K.T. performed the experiments and the characterization, analyzed the data. The manuscript was written through contributions of all of the authors. All of the authors have approved the final version of the manuscript.

Acknowledgments: The authors are thankful to Marmara University Nanotechnology and Biomaterial Research and Implementation Centre for their support.

Conflicts of Interest: The authors declare no conflict of interest.

References

1. Komur, B.; Bayrak, F.; Ekren, N.; Eroglu, M.; Oktar, F.; Sinirlioglu, Z.; Yucel, S.; Guler, O.; Gunduz, O., Starch/PCL composite nanofibers by co-axial electrospinning technique for biomedical applications. *Biomedical engineering online* **2017,** *16* (1), 40.
2. Paneva, D.; Manolova, N.; Argirova, M.; Rashkov, I., Antibacterial electrospun poly (ε-caprolactone)/ascorbyl palmitate nanofibrous materials. *International journal of pharmaceutics* **2011,** *416* (1), 346-355.
3. Hou, Q.; Grijpma, D. W.; Feijen, J., Preparation of Porous Poly (ε-caprolactone) Structures. *Macromolecular rapid communications* **2002,** *23* (4), 247-252.
4. Patil, P. T.; Anwane, R. S.; Kondawar, S. B., Development of electrospun polyaniline/ZnO composite nanofibers for LPG sensing. *Procedia Materials Science* **2015,** *10*, 195-204.
5. Virovska, D.; Paneva, D.; Manolova, N.; Rashkov, I.; Karashanova, D., Electrospinning/electrospraying vs. electrospinning: a comparative study on the design of poly (l-lactide)/zinc oxide non-woven textile. *Applied Surface Science* **2014,** *311*, 842-850.
6. Dobrzański, L.; Hudecki, A.; Chladek, G.; Król, W.; Mertas, A., Surface properties and antimicrobial activity of composite nanofibers of polycaprolactone with silver precipitations. *Archives of Materials Science and Engineering* **2014,** *70* (2), 53-60.
7. Uğur Kaya, A.; Güner, S.; Esmer, K., Effects of solution mixing temperature on dielectric properties of PMMA/Pristine bentonite nanocomposites. *Journal of Applied Polymer Science* **2014,** *131* (4).
8. Kaya, A. U.; Esmer, K.; Tekin, N.; Beyaz, S. K., Investigation of temperature, thermodynamic parameters and dielectrical properties of poly (vinylimidazole)–Na–bentonite nanocomposite. *Journal of Applied Polymer Science* **2011,** *120* (2), 874-879.
9. Augustine, R.; Kalarikkal, N.; Thomas, S., Electrospun PCL membranes incorporated with biosynthesized silver nanoparticles as antibacterial wound dressings. *Applied Nanoscience* **2016,** *6* (3), 337-344.
10. Augustine, R.; George, S. C.; Kalarikkal, N.; Thomas, S., Gentamicin loaded electrospun poly (ε-caprolactone)/TiO2 nanocomposite membranes with antibacterial property against methicillin resistant Staphylococcus aureus. *Polymer-Plastics Technology and Engineering* **2016,** *55* (17), 1785-1796.

11. Elumalai, K.; Velmurugan, S.; Ravi, S.; Kathiravan, V.; Ashokkumar, S., Bio-fabrication of zinc oxide nanoparticles using leaf extract of curry leaf (Murraya koenigii) and its antimicrobial activities. *Materials Science in Semiconductor Processing* **2015,** *34*, 365-372.
12. Raheman, F.; Deshmukh, S.; Ingle, A.; Gade, A.; Rai, M., Silver nanoparticles: novel antimicrobial agent synthesized from an endophytic fungus Pestalotia sp. isolated from leaves of Syzygium cumini (L). *Nano Biomed Eng* **2011,** *3* (3), 174-178.
13. Aydogdu, M. O.; Ekren, N.; Suleymanoglu, M.; Erdem-Kuruca, S.; Lin, C.-C.; Bulbul, E.; Erdol, M. N.; Oktar, F. N.; Terzi, U. K.; Kilic, O., Novel electrospun polycaprolactone/graphene oxide/Fe3O4 nanocomposites for biomedical applications. *Colloids and Surfaces B: Biointerfaces* **2018,** *172*, 718-727.